




Article

Enhancing the Decolorization of Methylene Blue Using a Low-Cost Super-Absorbent Aided by Response Surface Methodology

Nor Hakimin Abdullah ^{1,*}, Mazlan Mohamed ¹, Norshahidatul Akmar Mohd Shohaimi ², Azwan Mat Lazim ³, Ahmad Zamani Abdul Halim ⁴, Nurasmah Mohd Shukri ⁵ and Mohammad Khairul Azhar Abdul Razab ^{5,*}

¹ Advanced Materials Research Cluster (AMRC), Faculty of Bioengineering and Technology, Universiti Malaysia Kelantan (UMK), Jeli 17600, Kelantan, Malaysia; mazlan.m@umk.edu.my

² Faculty of Applied Sciences, Universiti Teknologi MARA Pahang, Bandar Tun Razak 26400, Pahang, Malaysia; akmarshohaimi@uitm.edu.my

³ Department of Chemical Sciences, Faculty of Science and Technology, Universiti Kebangsaan Malaysia, Bangi 43600, Selangor, Malaysia; azwanlazim@ukm.edu.my

⁴ Faculty of Industrial Sciences and Technology, College of Computing and Applied Science, Universiti Malaysia Pahang, Gambang, Kuantan 26300, Pahang, Malaysia; ahmadzamani@ump.edu.my

⁵ School of Health Sciences, Universiti Sains Malaysia, Kubang Kerian 16150, Kelantan, Malaysia; nurasmah@usm.my

* Correspondence: norhakimin@umk.edu.my (N.H.A.); khairul.azhar@usm.my (M.K.A.A.R.); Tel.: +6014-8787153 (N.H.A.); +6013-9292848 (M.K.A.A.R.)



Citation: Abdullah, N.H.; Mohamed, M.; Mohd Shohaimi, N.A.; Mat Lazim, A.; Abdul Halim, A.Z.; Mohd Shukri, N.; Abdul Razab, M.K.A. Enhancing the Decolorization of Methylene Blue Using a Low-Cost Super-Absorbent Aided by Response Surface Methodology. *Molecules* **2021**, *26*, 4430. <https://doi.org/10.3390/molecules26154430>

Academic Editor: João Valente Nabais

Received: 30 May 2021

Accepted: 13 July 2021

Published: 22 July 2021

Publisher's Note: MDPI stays neutral with regard to jurisdictional claims in published maps and institutional affiliations.



Copyright: © 2021 by the authors. Licensee MDPI, Basel, Switzerland. This article is an open access article distributed under the terms and conditions of the Creative Commons Attribution (CC BY) license (<https://creativecommons.org/licenses/by/4.0/>).

Abstract: The presence of organic dyes from industrial wastewater can cause pollution and exacerbate environmental problems; therefore, in the present work, activated carbon was synthesized from locally available oil palm trunk (OPT) biomass as a low-cost adsorbent to remove synthetic dye from aqueous media. The physical properties of the synthesized oil palm trunk activated carbon (OPTAC) were analyzed by SEM, FTIR-ATR, and XRD. The concurrent effects of the process variables (adsorbent dosage (g), methylene blue (MB) concentration (mg/L), and contact time (h)) on the MB removal percentage from aqueous solution were studied using a three-factor three-level Box–Behnken design (BBD) of response surface methodology (RSM), followed by the optimization of MB adsorption using OPTAC as the adsorbent. Based on the results of the analysis of variance (ANOVA) for the three parameters considered, adsorbent dosage (X_1) is the most crucial parameter, with an F -value of 1857.43, followed by MB concentration (X_2) and contact time (X_3) with the F -values of 95.60 and 29.48, respectively. Furthermore, the highest MB removal efficiency of 97.9% was achieved at the optimum X_1 , X_2 , and X_3 of 1.5 g, 200 mg/L, and 2 h, respectively.

Keywords: activated carbon; agriculture waste; methylene blue; optimization; wastewater treatment

1. Introduction

Over one third quarter of the Earth's surface consists of water. Today, rivers and oceans face environmental issues related to water pollution and contamination, with textile industries as the primary source of these issues. More than 8000 chemicals used in the textile industry are harmful and poisonous to human health and aquatic ecological systems [1]. Even worse, the environmental pollution of rivers and soils by dyes could directly interfere with the photosynthesis process, leading to increased toxicity of living beings [2]. Moreover, the environmental problems could worsen due to high levels of heavy metals in dyes (e.g., zinc, lead, copper, mercury, and nickel) [3]. Thus, several reliable methods have been studied for colored wastewater treatment, namely flocculation [4–6], coagulation [7–9], membrane separation [10,11], bacterial strains [4], and adsorption [12–14].

Adsorption involves the adhesion of substances present in a liquid phase onto a solid surface [15]. Colored water is commonly treated using adsorption, which offers

several advantages, being a straightforward and low-cost process, as well as having a high efficiency and versatility [16–18]. The adsorption and removal of dyes from wastewater is usually performed using activated carbon (AC) due to various benefits of employing AC containing a high carbon content, including simple operation, high porosity, and adsorption capacity [19,20]. AC can be prepared from agriculture biomass, such as coconut shell [21,22], corncob [23], durian shell [24,25], and oil palm [26,27]. Many solid wastes from different parts of the oil palm, including trunks, fibers, and empty fruit bunches, are produced in Malaysia, and these parts are good sources for producing AC [28]. Oil palm trunk (OPT) consists of 22.6% lignin, 21.2% hemicellulose, 39.9% cellulose, 1.9% ash, 3.1% wax, and 11.3% other constituents, which would be beneficial as raw materials to prepare AC as an adsorbent [29]. The conversion of OPT as an agricultural waste into a new, beneficial product would reduce environmental impacts, and this approach is in line with the waste-to-wealth concept.

A three-level factorial design is needed for the Box–Behnken design (BBD) of response surface methodology (RSM) when conducting an experiment. BBD–RSM can be implemented to obtain optimum adsorption conditions with the minimum number of experiments and least amount of chemicals. This approach can also be applied for the investigation of the effect of independent variables (factors) on the process and their influence on a dependent variable (response) [30]. BBD–RSM has been used to optimize adsorbate removal using AC prepared from agriculture waste [31–36], zeolite [37], and biopolymers [38]. Nevertheless, to the best of the authors' knowledge, no study has been conducted for the optimization of synthetic dye removal using AC prepared from OPT.

In this study, OPT was used as a raw material for the preparation of oil palm trunk activated carbon (OPTAC), which was then characterized using scanning electron microscopy (SEM), Fourier transform infrared-attenuated total reflection (FTIR-ATR), and X-ray diffraction (XRD). Methylene blue (MB) removal was conducted to evaluate the adsorption capacity of OPTAC. Ultraviolet-visible (UV-vis) spectroscopy was applied to optimize the MB removal, based on a full-factorial experimental design. The effect of independent variables (adsorbent dosage, MB concentration, and contact time) on the MB removal percentage from aqueous solution was studied by utilizing OPTAC as the adsorbent. Moreover, a BBD design was utilized to determine the optimal MB removal and investigate the relationship between independent variables and MB removal.

2. Results

2.1. Characterization of OPTAC

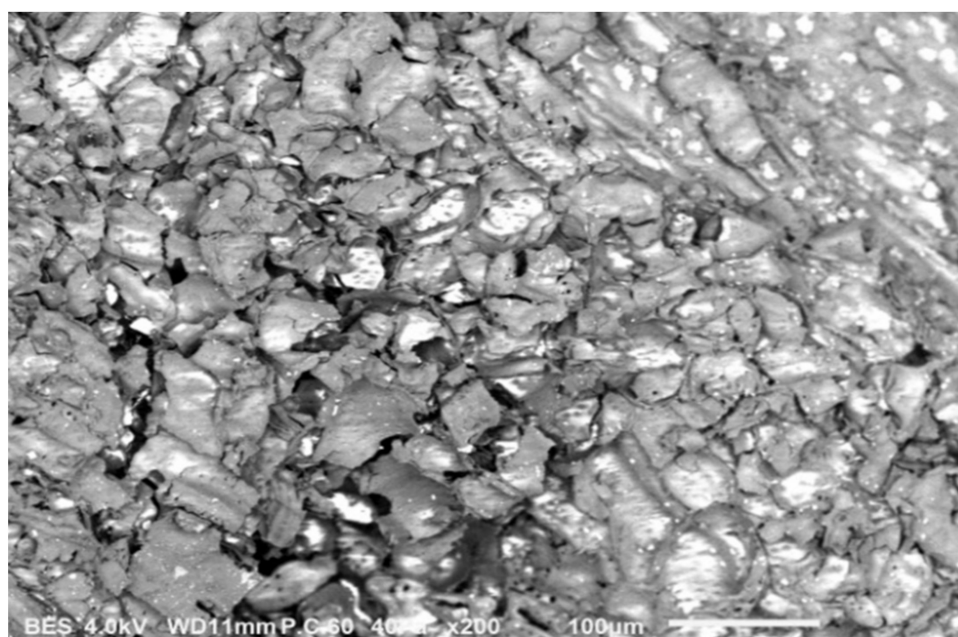
2.1.1. Scanning Electron Microscopy

Figure 1 presents the surface morphology of the native and activated carbon produced using OPT. No distinct pores could be observed on the surface of the OPT before chemical activation (Figure 1a). Meanwhile, good pore formation could be observed on the prepared OPTAC of different shapes and sizes (Figure 1b–d). Chemical activation eased the enlargement of pores in the carbon structure [39] and the pore development on the AC surface due to the evaporation of H_3PO_4 during carbonization [40]. The most noticeable changes that occurred after the activation were cracks and basic pores due to the volatilization of cellulose, hemicellulose, lignin content, and moisture of the carbon [41]. The successful activation process and the porous structure of the OPTAC will improve the efficiency of the adsorption process.

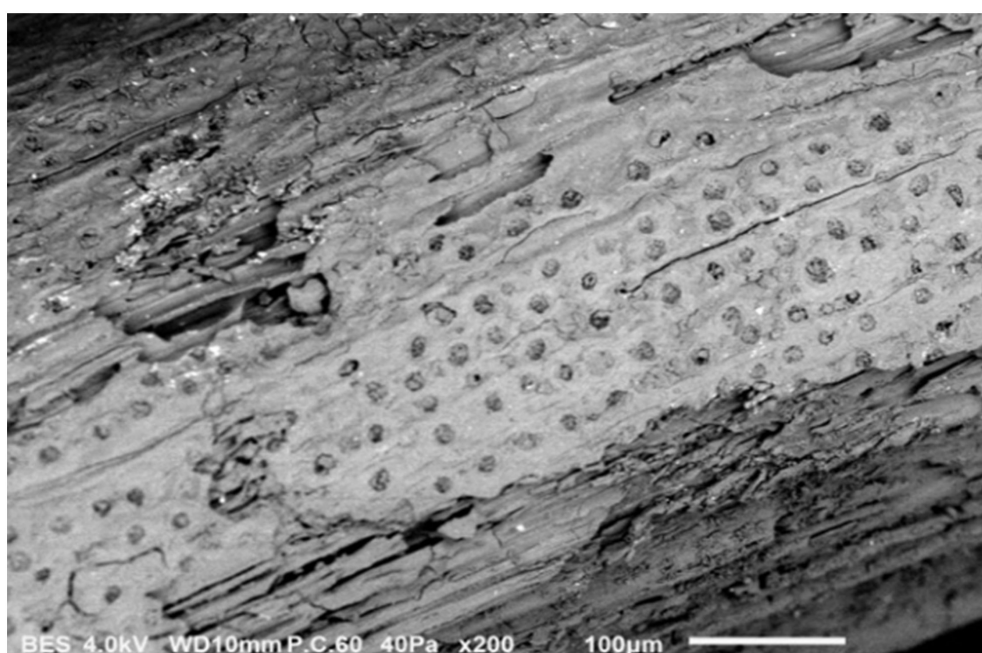
2.1.2. FTIR-ATR Spectra of OPTAC

The FTIR-ATR spectra of the native and activated carbon of OPT are presented in Figure 2, where significant changes can be seen by comparing the spectra of native carbon (NC) (Figure 2a) and OPTAC (Figure 2b). The spectrum of NC of OPT consists of several significant peaks at 3353.3 cm^{-1} , suggesting the characteristic absorption peak of O–H and N–H symmetric stretching vibration, 2111.5 cm^{-1} for $\text{C}\equiv\text{C}$ stretching vibration of alkynes, 1574.2 cm^{-1} denoting C=O and C=C stretching vibrations, 1372.6 cm^{-1} (carboxylic acid

O-H), 1119 cm^{-1} for C-H in-plane deformation, and 749 cm^{-1} showing C-H symmetric stretching vibration [42]. There are slight additions and changes in the FTIR-ATR spectrum for OPTAC compared to NC due to the acidic activation process, which modified its surface properties. The chemical treatment of OPTAC altered its carboxylate group, which explains the disappearance of the peak at 1372 cm^{-1} for the spectrum of OPTAC, whereas the appearance of peaks at 1796.2 cm^{-1} (stretching vibration of C=O in -COOH), 1557.5 cm^{-1} (assignable to stretching vibration of C=C), and 953 cm^{-1} correspond to the stretching vibration of C-O, C-X, or C-C [43]. The OPTAC spectrum has fewer strong peaks due to the heating effect during the activation process, where the decomposition of lignin, cellulose, and hemicellulose took place [44].



(a)

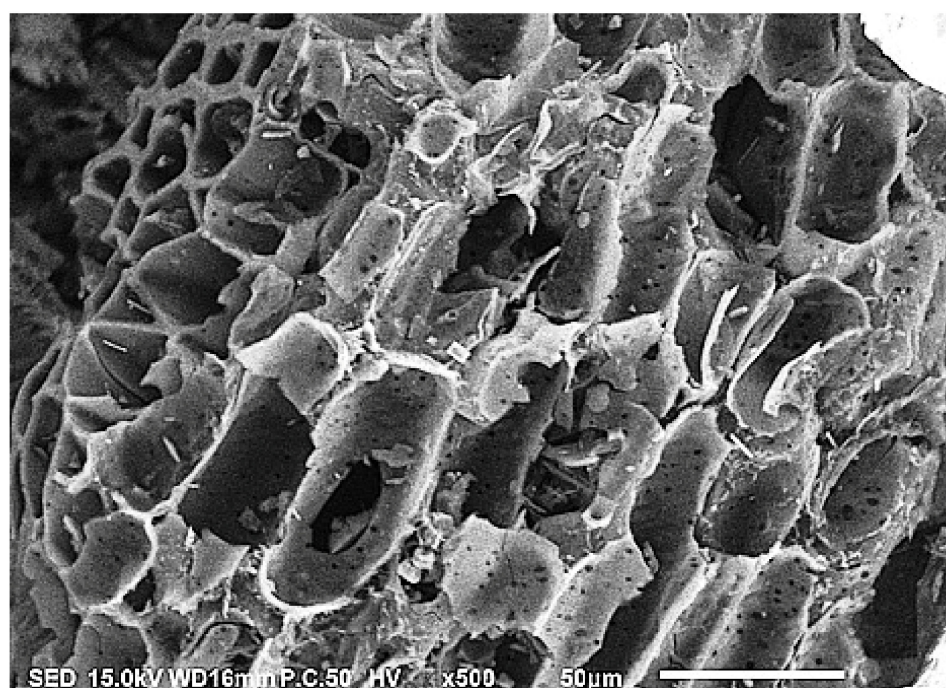


(b)

Figure 1. Cont.



(c)



(d)

Figure 1. SEM images indicating carbon before activation (a), and after activation with H_3PO_4 (b), (c), and (d).

2.1.3. XRD of OPTAC

Figure 3 exhibits the XRD results for native carbon (NC) and OPTAC. The weak and broad patterns near $2\theta = 24^\circ$ and $2\theta = 43^\circ$ in the spectra are due to the amorphous phase of the samples [45]. In addition, broad diffraction was observed in all samples near $2\theta = 24^\circ$ due to the microcrystalline graphite multilayers [46].

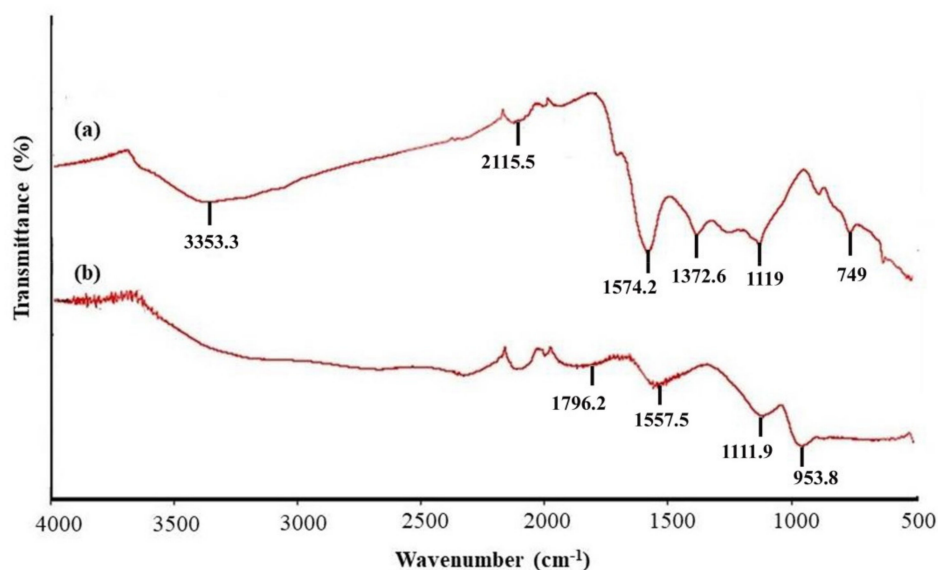


Figure 2. FTIR-ATR spectra for (a) NC and (b) OPTAC.

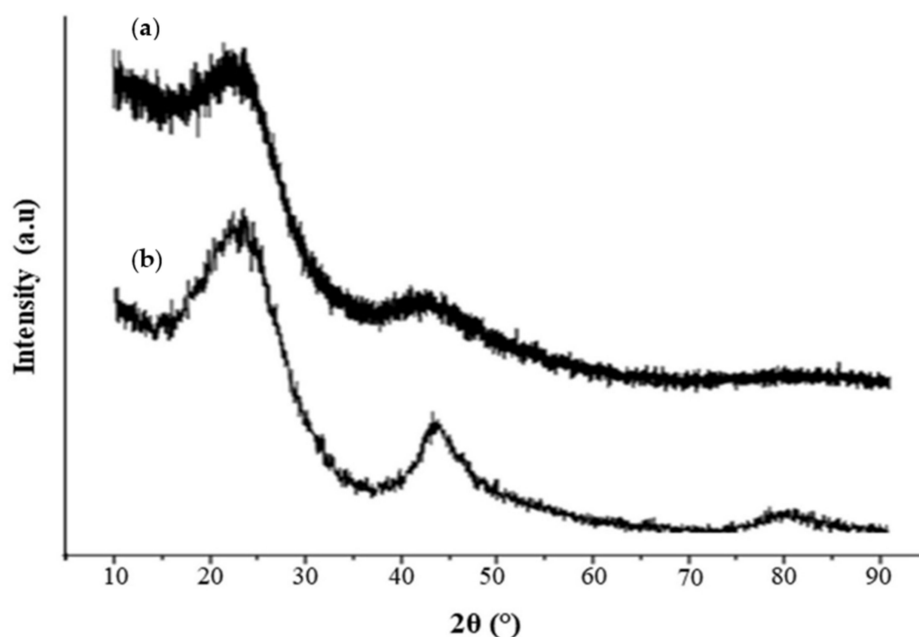


Figure 3. X-ray diffraction patterns of (a) NC and (b) OPTAC.

2.2. Response Surface Methodology–Box–Behnken Design

Table 1 presents the experimental results obtained by studying MB removal optimization using the BBD, where 17 experimental runs were performed randomly. Three independent variables (adsorbent dosage, MB concentration, and contact time) were selected to determine the most influential factors for MB removal. The experimental results based on the full-factorial BBD were fitted to the quadratic equation using multiple regression analysis. The quadratic model for MB removal (response) as a function of three independent variables is shown in Equation (1):

$$\text{MB Removal (Y)} = 94.86 + 18.78 * X_1 - 4.26 * X_2 + 2.37 * X_3 + 1.54 * X_1 * X_2 - 0.39 * X_1 * X_3 + 2.09 * X_2 * X_3 - 11.50 * X_1^2 - 7.23 * X_2^2 - 7.43 * X_3^2 \quad (1)$$

where Y is the estimated response (MB removal), and X_1 , X_2 , and X_3 are the independent variables of adsorbent dosage, MB concentration, and contact time, respectively.

Table 1. Experimental and predicted results for MB removal.

Run	X_1 (g)	X_2 (mg/L)	X_3 (h)	MB Removal (%)	
				Actual	Predicted
1	1	400	1	71.22	71.49
2	0.5	400	2	51.19	51.54
3	0.5	300	1	55.01	54.39
4	1	300	2	95.78	94.86
5	1	300	2	95.66	94.86
6	1.5	300	1	91.9	92.74
7	1	200	3	85.01	84.74
8	0.5	300	3	60.74	59.9
9	0.5	200	2	62.05	63.15
10	1.5	200	2	97.98	97.63
11	1.5	400	2	93.3	92.2
12	1	300	2	93.67	94.86
13	1	400	3	79.91	80.39
14	1	300	2	93.57	94.86
15	1	200	1	84.67	84.19
16	1.5	300	3	96.07	96.69
17	1	300	2	95.64	94.86

Table 2 presents the ANOVA results based on the developed quadratic model for MB removal under the designated experimental conditions. From the results, the model is significant, with the model F -value of 304.23 and p -value of 0.001. In addition, noise contributed to 0.01% probability of the model F -value. According to the findings, X_1 was the most influential parameter, with an F -value of 1,857.43, followed by X_2 , with an F -value of 95.60. The least influential parameter was X_3 , with an F -value of 29.48. The model is significant if the p -value is less than 0.05. The obtained lack-of-fit value of 1.82 proved that the lack-of-fit is not important compared to the pure error. The lack of fit had a 36.36 percent chance of occurring due to noise. The model was good and fit well based on the insignificant lack-of-fit. Furthermore, the response was significantly influenced by the interaction between X_1X_2 and X_2X_3 , according to the significance of the model (i.e., p -value) set at 0.05.

Table 2. ANOVA results for MB removal.

Source	Sum of Squares	Degree of Freedom	Mean Square	F -Value	p -Value
Model	4160.28	9	462.25	304.23	<0.0001
X_1	2822.26	1	2822.26	1857.43	<0.0001
X_2	145.27	1	145.27	95.60	<0.0001
X_3	44.79	1	44.79	29.48	0.0010
X_1X_2	9.55	1	9.55	6.28	0.0406
X_1X_3	0.61	1	0.61	0.40	0.5470
X_2X_3	17.43	1	17.43	11.47	0.0116
X_1^2	557.16	1	557.16	366.69	<0.0001
X_2^2	220.14	1	220.14	144.88	<0.0001
X_3^2	232.49	1	232.49	153.0	<0.0001
Residual	10.64	7	1.52		
Lack of Fit	5.46	3	1.82	1.41	0.3636
Pure Error	5.17	4	1.29		
Std. Dev.	1.23	16	R^2	0.9974	
Mean	82.55		Adj R^2	0.9942	
			Predicted R^2	0.9771	

The coefficient of determination (R^2) of 0.9974 indicates that the projected polynomial model fits the data tolerantly well. The predicted R^2 (Pred R-Sq) value of 0.9771 agreed reasonably with the adjusted R^2 (Adj R-Sq) value of 0.9942. Figure 4 shows a comparison of the predicted and actual percentages of MB removal. The predicted and actual values are in good agreement as the values are distributed along the regression line; furthermore, the values did not exceed the experimental range [47].

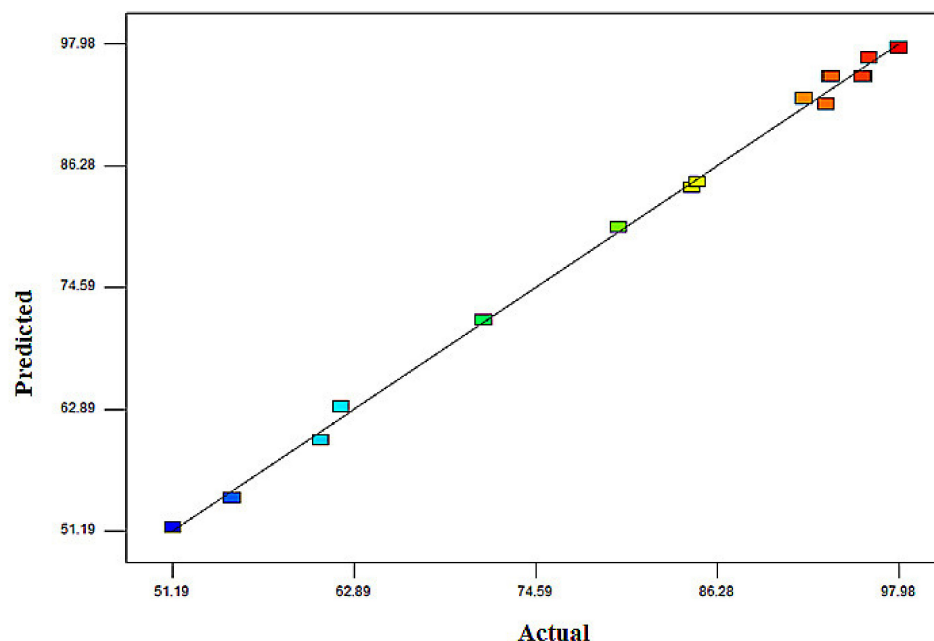
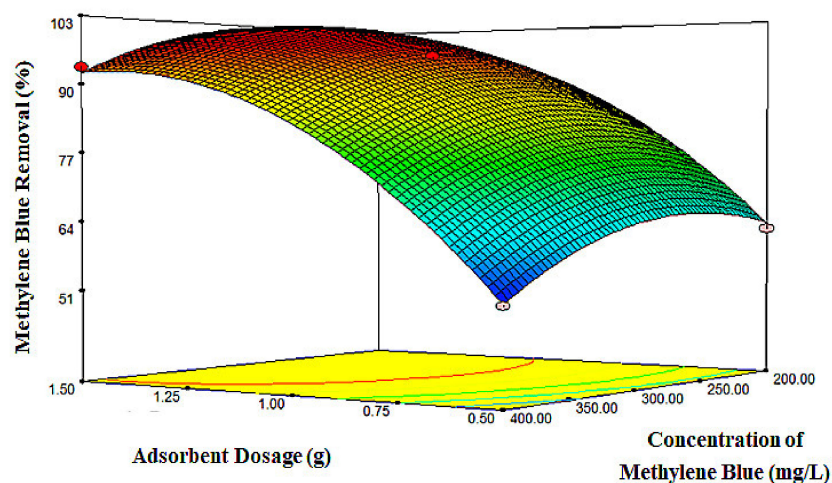


Figure 4. Correlation of predicted versus actual responses for the MB removal percentage.

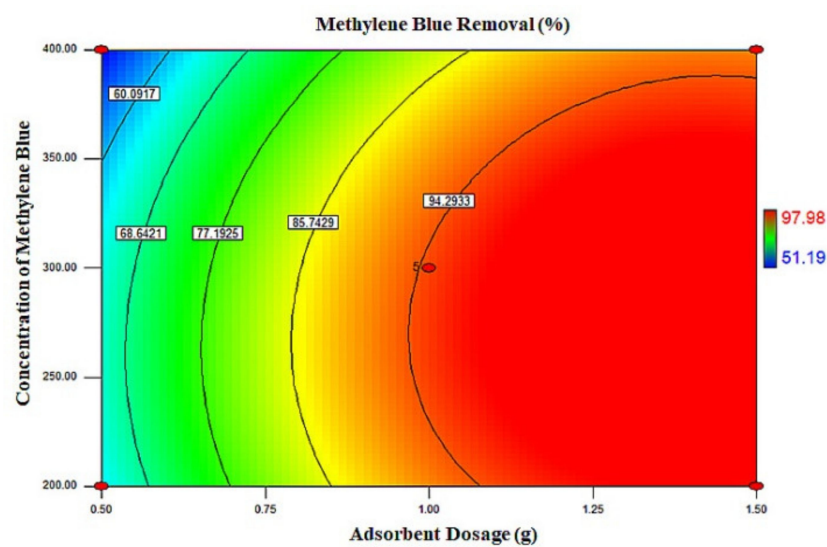
2.3. Response Surface Plots

Three-dimensional (3D) and two-dimensional (2D) plots were produced using Design Expert 7.0. The plots highlight the relationship between independent variables (X_1 , X_2 , and X_3) and the response (MB removal), as presented in Figures 5–7. For both contour and surface plots, two continuous variables were varied with MB removal as the response, while another variable was fixed at a zero level. Referring to Figure 5, the adsorbent dosage and MB concentration were varied, whereas the contact time was fixed at 2 h. The results clearly showed that the maximum MB removal obtained was 97.98% at approximately 1.5 g of adsorbent dosage and 200 ppm of dye concentration within 2 h. By increasing the adsorbent dosage, the adsorption efficiency increased significantly, as there was more available surface area and active sites and an increase of vacant sites for the adsorption of MB molecules on the adsorbent [48].

The behavior of MB removal, influenced by varied adsorbent dosages and contact times with the dye concentration fixed at 300 mg/L, is presented in Figure 6. The maximum MB adsorption (i.e., 96.07%) was obtained at a higher contact time. In the dye adsorption process by the adsorbent, first, the adsorbate would reach the boundary layer, before diffusing into the adsorbent surface, and later into the porous adsorbent structure, thus explaining the lengthy adsorption process [48]. The effect of different contact times and MB concentrations on MB removal is presented in Figure 7, with the adsorbent dosage set at a zero level. It could be observed that the percentage of MB removal increased as the MB concentration and contact time increased from 200 to 300 mg/L and from 1 to 2 h, respectively. Moreover, within those levels, the MB removal reached its maximum value.

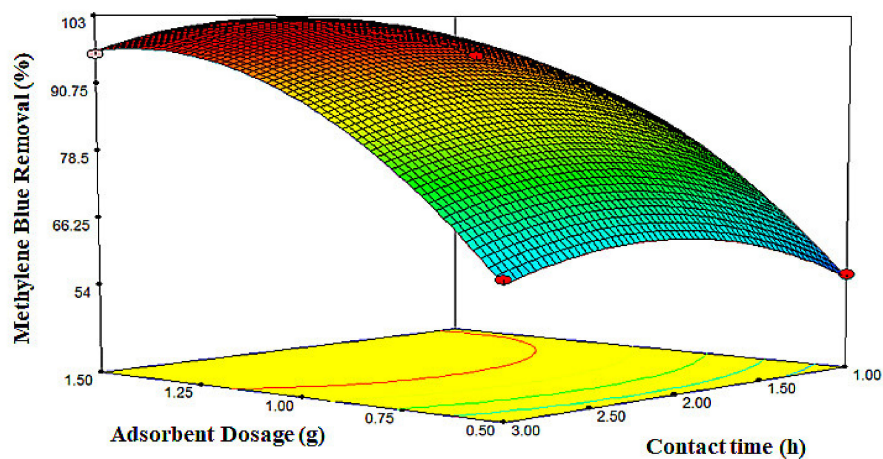


(a)



(b)

Figure 5. (a) 3D surface plot and (b) 2D contour plot for the effect of adsorbent dosage and MB concentration on MB removal percentage.



(a)

Figure 6. Cont.

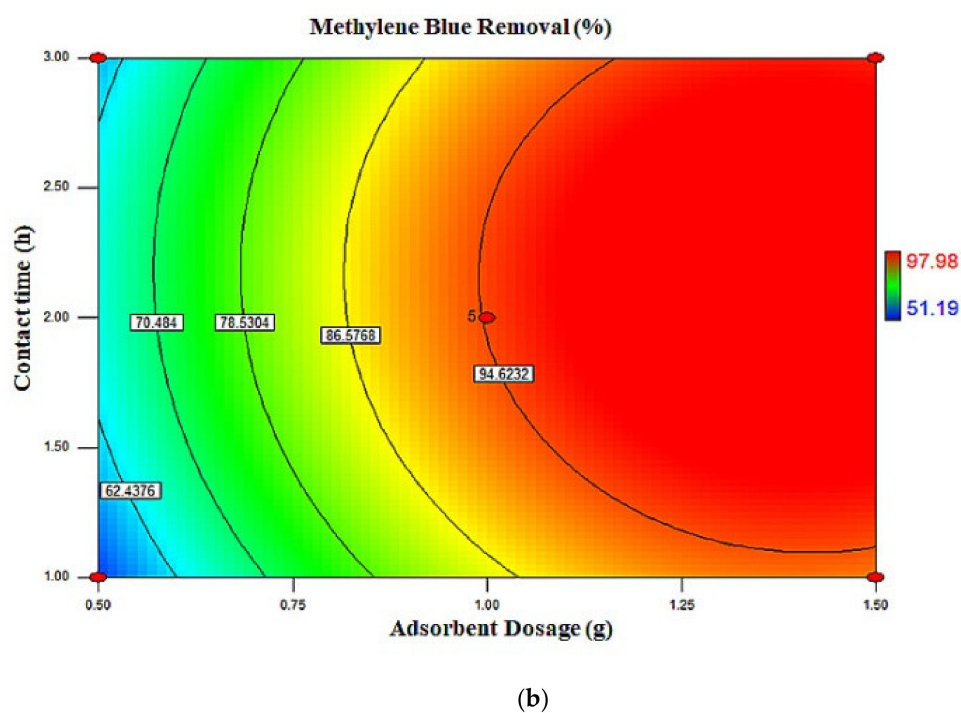


Figure 6. (a) 3D surface plot and (b) 2D contour plot for the effect of adsorbent dosage and contact time on MB removal percentage.

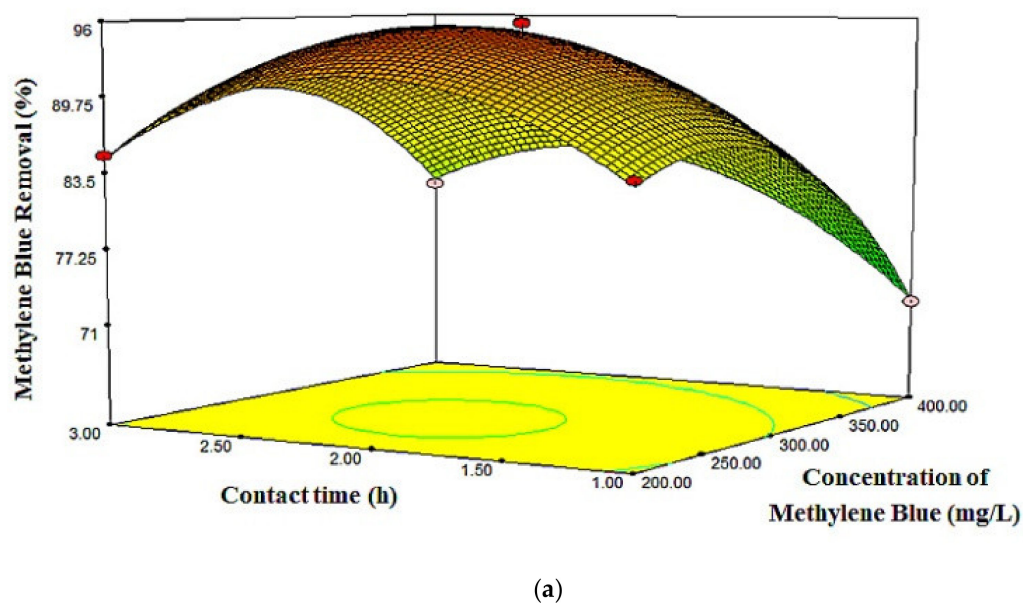


Figure 7. Cont.

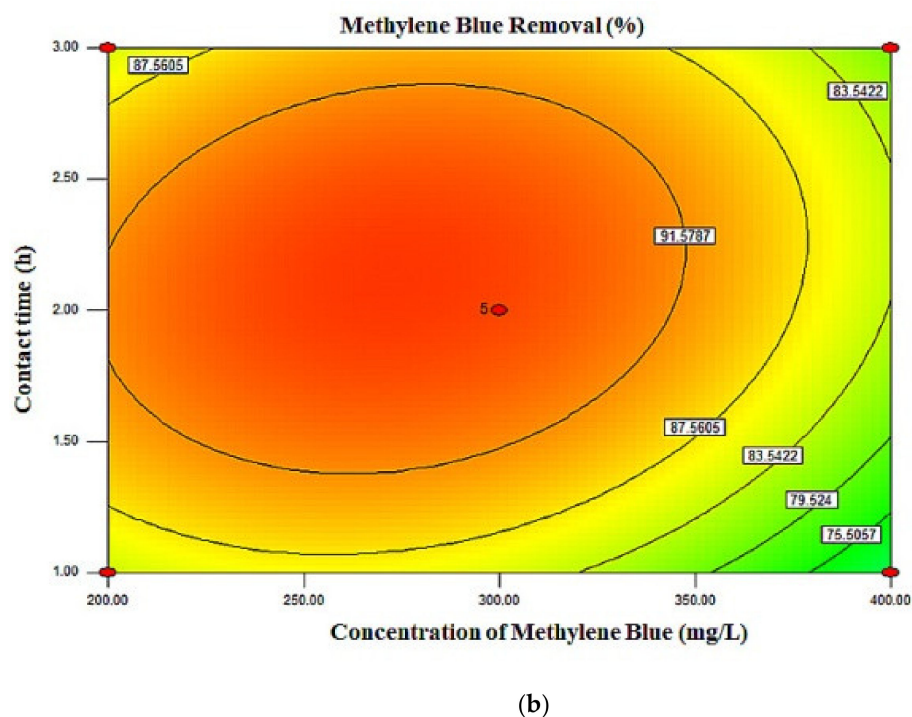


Figure 7. (a) 3D surface plot and (b) 2D contour plot for the effect of MB concentration and contact time on MB removal percentage.

To obtain the maximum MB elimination, the experiment was validated at the optimal settings, as seen in Table 3. Based on the initial parameters set to obtain the optimum response ($X_1 = 1.5$ g, $X_2 = 200$ mg/L, and $X_3 = 2$ h), the estimated MB removal was 95.5%, which was obtained at the optimum conditions of $X_1 = 1.25$ g, $X_2 = 350$ mg/L, and $X_3 = 2.15$ h, as shown in Table 4. An additional experiment was performed to validate the optimum conditions and the model agreement. From the results, the MB removal achieved was 97.75%, with a maximum error of only $\pm 2.3\%$. Hence, this small error reflects the validity of the response surface optimization conducted [49].

Table 3. Experimental ranges and levels of independent variables.

Independent Variables	Range and Level		
	−1	0	1
Adsorbent Dosage, X_1 (g)	0.5	1	1.5
MB Concentration, X_2 (mg/L)	200	300	400
Contact Time, X_3 (h)	1	2	3

Table 4. Values of process parameters for the maximum MB removal percentage.

Parameters	Values
Percentage of MB Removal (%)	95.50
X_1 (Adsorbent Dosage, g)	1.25
X_2 (MB Concentration, mg/L)	350
X_3 (Contact Time, h)	2.15

3. Materials and Methods

All chemical reagents were of analytical grade and used without further purification. Oil palm trunk chips were purchased from a local factory. Phosphoric acid (H_3PO_4 , 80%) and MB were purchased from Sigma-Aldrich, (Petaling Jaya, Malaysia).

The surface morphology of oil palm trunk activated carbon (OPTAC) was characterized using a scanning electron microscope (model JSM-5910, JEOL USA, Peabody, MA, USA). A Nicolet iS20 spectrophotometer was used for the identification of chemical functional groups present in OPTAC through FTIR-ATR analysis. Meanwhile, a Bruker D2 Phase X-ray diffractometer with Cu-K α ($\lambda = 0.154060 \text{ \AA}$) radiation source operating at 40 kV and 25 mA was utilized for studying the diffraction patterns of OPTAC. A UV-vis spectrophotometer (HACH DR6000) was used for the determination of MB removal percentage.

3.1. Preparation of OPTAC

First, water-soluble organic compounds were removed from OPT by rinsing the OPT several times with distilled water. Next, the sample was ground and sieved using a 0.5 mm sieve to obtain a uniform-sized sample followed by a pre-carbonization process for the sieved OPT in a furnace for 3 h at 350 °C. Subsequently, the sample was soaked in H₃PO₄ with a ratio of 1:10 (*w/w*) for 12 h and the mixture was stirred at 70 °C until the excess phosphoric acid was evaporated. The sample then was placed in an oven at 120 °C for an additional 12 h. Upon completion, the sample was heated in a furnace at 500 °C and 3 h for carbonization; subsequently, the sample was washed thoroughly and repeatedly using distilled water and basic solution to obtain a neutral pH. Lastly, the sample was inserted into an oven for drying at 120 °C for 12 h. The dried sample was kept in an airtight container prior to further use.

3.2. Dye Adsorption Study

In this study, MB was used as the adsorbate. The determined concentration of MB was placed in a 250-mL beaker and the prepared OPTAC was added to the beaker. Stirring was maintained at a stirring speed of 300 rpm and a temperature of 30 °C. A fixed volume of MB solution was collected at the determined contact time interval during each adsorption experiment to evaluate the amount of MB removed. The absorbance measurement of MB solution was conducted using a HACH DR6000 spectrophotometer at a wavelength of 662 nm. Equation (2) was used to calculate the MB removal percentage:

$$\text{MB Removal (\%)} = \frac{C_0 - C_i}{C_0} \quad (2)$$

where C_0 and C_i (mg/L) are the initial concentration and concentration at time t , respectively.

3.3. Design of Experiment

Three independent variables (adsorbent dosage, X_1 (g); MB concentration, X_2 (mg/L); and contact time, X_3 (h)) influencing MB removal from aqueous solution were evaluated by adopting a BBD, with MB removal percentage as the response. The actual and coded levels of independent variables used in the experimental design are presented in Table 3. The experimental design matrix was created using Design Expert 7.0 according to 33 factorial designs.

All experiments were carried out randomly to reduce the impact of systematic errors on the observed responses. For each component evaluated, a second-order polynomial equation was fitted as a function of X , as shown in Equation (3):

$$Y = \beta_0 + \sum_{i=1}^3 \beta_i X_i + \sum_{i=1}^3 \beta_{ii} X_i^2 + \sum_{\substack{i=1 \\ 1 < j}}^3 \beta_{ij} X_i X_j \quad (3)$$

where Y is the predicted response (MB removal, %); β_0 , β_i , β_{ii} , and β_{ij} are the model regression coefficients; and X_i and X_j represent the independent variables ($i \neq j$). The effect of each independent variable on the response was evaluated using the model, as well as the optimum response (Y_{opt}) and corresponding independent variables.

Analysis of variance (ANOVA) was performed to check the model's validity, where the analysis enables the determination of the relationship between the response and the process variables based on the proposed model. Meanwhile, the Fisher *F*-distribution test and *p*-value were used for evaluating the model's statistical significance [50].

4. Conclusions

This research demonstrated that AC as an adsorbent was successfully synthesized from oil palm trunk (OPT). The characterization of the synthesized OPTAC using SEM revealed its porous structure. Meanwhile, the FTIR-ATR and XRD spectra showed a successful activation process and an amorphous phase of OPTAC were obtained, respectively. The optimization of methylene blue (MB) removal was carried out using a Box–Behnken design (BBD) of RSM for three independent variables (adsorbent dosage, MB concentration, and contact time). From the ANOVA results, an MB removal of up to 97.9% was obtained at the optimum conditions of $X_1 = 1.5$ g, $X_2 = 200$ mg/L, and $X_3 = 2$ h. Adsorbent dosage was the most influential parameter among the independent variables considered. Based on the verification experiment performed at the optimum conditions, the experimental MB removal (97.75%) closely agreed with the predicted MB removal (95.5%). Therefore, it can be concluded that the OPTAC prepared from agricultural waste is an excellent candidate as a low-cost adsorbent in the removal of contaminants from an aqueous solution.

Author Contributions: Conceptualization, supervision of the experiments, and wrote the original author contributions: manuscript, N.H.A.; Methodology and project administration, M.M.; Methodology and formal analysis, N.A.M.S.; Reviewing and editing the manuscript, A.M.L.; Methodology and validation, A.Z.A.H.; Methodology and resources, N.M.S.; Resources, reviewing, and editing the manuscript, M.K.A.A.R. All authors have read and agreed to the published version of the manuscript.

Funding: This work was funded by Universiti Malaysia Kelantan through the SGJP research grant scheme R/SGJP/A13.00/00462A/001/2018/000481 and Short Term Research Grant, Universiti Sains Malaysia [304/PPSK/6315499].

Institutional Review Board Statement: Not applicable.

Informed Consent Statement: Not applicable.

Data Availability Statement: All data is contained within the article.

Conflicts of Interest: The authors declare no conflict of interest.

Sample Availability: Samples of the compounds are not available from the authors.

References

1. Al-Ghouti, M.A.; Sweleh, A.O. Optimizing textile dye removal by activated carbon prepared from olive stones. *Environ. Technol. Innov.* **2019**, *16*, 100488. [[CrossRef](#)]
2. Samarbaf, S.; Tahmasebi, B.Y.; Yazdani, M.; Babaei, A.A. A comparative removal of two dyes from aqueous solution using modified oak waste residues: Process optimization using response surface methodology. *J. Ind. Eng. Chem.* **2019**, *73*, 67–77. [[CrossRef](#)]
3. Koo, W.K.; Gani, N.A.; Shamsuddin, M.S.; Subki, N.S. Comparison of Wastewater Treatment using Activated Carbon from Bamboo and Oil Palm: An Overview. *J. Trop. Resour. Sustain. Sci.* **2015**, *3*, 54–60.
4. Favero, B.M.; Favero, A.C.; Taffarel, S.R.; Souza, F.S. Evaluation of the efficiency of coagulation/flocculation and Fenton process in reduction of colour, turbidity and COD of a textile effluent. *Environ. Technol.* **2020**, *41*, 1580–1589. [[CrossRef](#)] [[PubMed](#)]
5. Ma, J.; Xia, W.; Fu, X. Magnetic flocculation of algae-laden raw water and removal of extracellular organic matter by using composite flocculant of Fe₃O₄/cationic polyacrylamide. *J. Clean. Prod.* **2020**, *248*, 119276. [[CrossRef](#)]
6. Wei, T.; Wu, L.; Yu, F. pH-responsive chitosan-based flocculant for precise dye flocculation control and the recycling of textile dyeing effluents. *RSC Adv.* **2018**, *8*, 39334–39340. [[CrossRef](#)]
7. Ilhan, F.; Ulucan-Altuntas, K.; Can, D.U.K. Treatability of raw textile wastewater using Fenton process and its comparison with chemical coagulation. *Desalin. Water Treat.* **2019**, *162*, 142–148. [[CrossRef](#)]
8. Vijayaraghavan, G.; Shanthakumar, S. Effective removal of Reactive Magenta dye in textile effluent by coagulation using algal alginate. *Desalin. Wat. Treat.* **2018**, *121*, 22–27. [[CrossRef](#)]
9. Oraeki, T.; Skouteris, G.; Ouki, S. Optimization of coagulation-flocculation process in the treatment of wastewater from the brick-manufacturing industry. *Water Pract. Technol.* **2018**, *13*, 780–793. [[CrossRef](#)]

10. Riaz, S.; Park, S.J. An overview of TiO₂-based photocatalytic membrane reactors for water and wastewater treatments. *J. Ind. Eng. Chem.* **2020**, *84*, 23–41. [[CrossRef](#)]
11. Shi, W.; Zeng, X.; Li, H.; Zhang, H.; Qin, X.; Zhou, R. Removal of dyes by poly (p -phenylene terephthamide)/polyvinylidene fluoride hollow fiber in-situ blend membranes. *J. Appl. Polym. Sci.* **2020**, *137*, 48569. [[CrossRef](#)]
12. Tara, N.; Siddiqui, S.I.; Rathi, G.; Chaudhry, S.A.; Inamuddin, A.A.M. Nano-engineered Adsorbent for the Removal of Dyes from Water: A Review. *Curr. Anal. Chem.* **2020**, *16*, 14–40. [[CrossRef](#)]
13. Patil, K.; Jeong, S.; Lim, H.; Byun, H.-S.; Han, S. Removal of volatile organic compounds from air using activated carbon impregnated cellulose acetate electrospun mats. *Environ. Eng. Res.* **2018**, *24*, 600–607. [[CrossRef](#)]
14. Senthil, K.P.; Joshiba, G.J.; Femina, C.C. A critical review on recent developments in the low-cost adsorption of dyes from wastewater. *Desalin. Water Treat.* **2019**, *172*, 395–416. [[CrossRef](#)]
15. Desta, M.B. Batch Sorption Experiments: Langmuir and Freundlich Isotherm Studies for the Adsorption of Textile Metal Ions onto Teff Straw (*Eragrostis tef*) Agricultural Waste. *J. Thermodyn.* **2013**, *2013*, 1–6. [[CrossRef](#)]
16. Hazzaa, R.; Hussein, M. Adsorption of cationic dye from aqueous solution onto activated carbon prepared from olive stones. *Environ. Technol. Innov.* **2015**, *4*, 36–51. [[CrossRef](#)]
17. Eris, S.; Azizian, S. Extension of classical adsorption rate equations using mass of adsorbent: A graphical analysis. *Sep. Purif. Technol.* **2017**, *179*, 304–308. [[CrossRef](#)]
18. Pardeep, S.; Pankaj, R.; Deepak; Pathania, G.S. Microwave induced KOH activation of guava peel carbon as an adsorbent for congo red dye removal from aqueous phase. *Indian J. Chem. Technol.* **2013**, *20*, 305–311.
19. Abdullah, N.H.; Ghani, N.A.A.; Razab, M.K.A.A. Methyl orange adsorption from aqueous solution by corn cob based activated carbon. *AIP Conf. Proc.* **2019**, *2068*, 20036.
20. Yahya, M.A.; Al-Qodah, Z.; Ngah, C.W.Z. Agricultural bio-waste materials as potential sustainable precursors used for activated carbon production: A review. *Renew. Sustain. Energy Rev.* **2015**, *46*, 218–235. [[CrossRef](#)]
21. Islam, M.A.; Ahmed, M.J.; Khanday, W.A.; Asif, M.; Hameed, B.H. Mesoporous activated coconut shell-derived hydrochar prepared via hydrothermal carbonization-NaOH activation for methylene blue adsorption. *J. Environ. Manag.* **2017**, *203*, 237–244. [[CrossRef](#)] [[PubMed](#)]
22. Arsyad, N.A.S.; Razab, M.K.A.A.; Noor, A.M.; Amini, M.H.M.; Yusoff, N.N.A.N.; Halim, A.Z.A.; Yusuf, N.A.A.N.; Masri, M.N.; Sulaiman, M.A.; Abdullah, N.H. Effect of chemical treatment on production of activated carbon from *Cocos nucifera* L. (Coconut) shell by microwave irradiation method. *J. Trop. Resour. Sustain. Sci.* **2016**, *4*, 112–116.
23. Yaseen, M.; Ullah, S.; Ahmad, W.; Subhan, S.; Subhan, F. Fabrication of Zn and Mn loaded activated carbon derived from corn cobs for the adsorptive desulfurization of model and real fuel oils. *Fuel* **2021**, *284*, 119102. [[CrossRef](#)]
24. Gopalakrishnan, Y.; Al-Gheethi, A.; Abdul Malek, M.; Marisa Azlan, M.; Al-Sahari, M.; Radin Mohamed, R.M.S.; Alkhadher, S.; Noman, E. Removal of Basic Brown 16 from Aqueous Solution Using Durian Shell Adsorbent, Optimisation and Techno-Economic Analysis. *Sustainability* **2020**, *12*, 8928. [[CrossRef](#)]
25. Tham, Y.J.; Latif, P.A.; Abdullah, A.M.; Taufiq-YA, Y.H. Physical Characteristics of Activated Carbon Derived from Durian Shell. *Asian J. Chem.* **2010**, *22*, 772–780.
26. Tran, T.D.H.; Charoensook, K.; Tai, H.C. Preparation of activated carbon derived from oil palm empty fruit bunches and its modification by nitrogen doping for supercapacitors. *J. Porous Mater.* **2021**, *28*, 9–18. [[CrossRef](#)]
27. Maulina, S.; Iriansyah, M. Characteristics of activated carbon resulted from pyrolysis of the oil palm fronds powder. *IOP Conf. Ser. Mater. Sci. Eng.* **2018**, *309*, 12072. [[CrossRef](#)]
28. Awalludin, M.F.; Sulaiman, O.; Hashim, R.; Nadhari, W.N.A.W. An overview of the oil palm industry in Malaysia and its waste utilization through thermochemical conversion, specifically via liquefaction. *Renew. Sustain. Energy Rev.* **2015**, *50*, 1469–1484. [[CrossRef](#)]
29. Yuliansyah, A.T.; Hirajima, T.; Kumagai, S.; Sasaki, K. Production of Solid Biofuel from Agricultural Wastes of the Palm Oil Industry by Hydrothermal Treatment. *Waste Biomass Valorization* **2010**, *1*, 395–405. [[CrossRef](#)]
30. Abdullah, N.H.; Wan Abu Bakar, W.A.; Hussain, R.; Bakar, M.B.; van Esch, J.H. Effect of homogeneous acidic catalyst on mechanical strength of trishydrazone hydrogels: Characterization and optimization studies. *Arab. J. Chem.* **2018**, *11*, 635–644. [[CrossRef](#)]
31. Lékéné, R.B.N.; Nsami, J.N.; Rauf, A. Optimization Conditions of the Preparation of Activated Carbon Based Egusi Seed Shells for Nitrate Ions Removal from Wastewater. *Am. J. Anal. Chem.* **2018**, *9*, 439–463. [[CrossRef](#)]
32. Inam, E.; Etim, U.J.; Akpabio, E.G.; Umoren, S.A. Process optimization for the application of carbon from plantain peels in dye abstraction. *J. Taibah Univ. Sci.* **2017**, *11*, 173–185. [[CrossRef](#)]
33. Daud, F.A.; Ismail, N.; Ghazi, R. Response Surface Methodology Optimization of Methylene Blue Removal by Activated Carbon Derived from Foxtail Palm Tree Empty Fruit Bunch. *J. Trop. Resour. Sustain. Sci.* **2016**, *4*, 25–30.
34. Radaei, E.; Moghaddam, M.R.A.; Arami, M. Removal of reactive blue 19 from aqueous solution by pomegranate residual-based activated carbon: Optimization by response surface methodology. *J. Environ. Health Sci. Eng.* **2014**, *12*, 65. [[CrossRef](#)] [[PubMed](#)]
35. Danish, M.; Khanday, W.A.; Hashim, R.; Sulaiman, N.S.B.; Akhtar, M.N.; Nizami, M. Application of optimized large surface area date stone (*Phoenix dactylifera*) activated carbon for rhodamin B removal from aqueous solution: Box-Behnken design approach. *Ecotoxicol. Environ. Saf.* **2017**, *139*, 280–290. [[CrossRef](#)]
36. Sadaf, S.; Bhatti, H.N.; Arif, M.; Amin, M.; Nazar, F.; Sultan, M. Box–Behnken design optimization for the removal of Direct Violet 51 dye from aqueous solution using lignocellulosic waste. *Desalin. Water Treat.* **2015**, *56*, 2425–2437. [[CrossRef](#)]

37. Shojaei, S.; Shojaei, S.; Pirkamali, M. Application of Box–Behnken Design Approach for Removal of Acid Black 26 from Aqueous Solution Using Zeolite: Modeling, Optimization, and Study of Interactive Variables. *Water Conserv. Sci. Eng.* **2019**, *4*, 13–19. [[CrossRef](#)]
38. Jawad, A.H.; Abdul Mubarak, N.S.; Nawawi, W.I. Optimization of Sorption Parameters for Color Removal of Textile Dye by Cross-linked Chitosan Beads Using Box-Behnken Design. *MATEC Web Conf.* **2016**, *47*, 5009. [[CrossRef](#)]
39. Bello, O.S.; Ahmad, M.A. Adsorptive removal of a synthetic textile dye using cocoa pod husks. *Toxicol. Environ. Chem.* **2011**, *93*, 1298–1308. [[CrossRef](#)]
40. Yakout, S.M.; Sharaf El-Deen, G. Characterization of activated carbon prepared by phosphoric acid activation of olive stones. *Arab. J. Chem.* **2016**, *9*, S1155–S1162. [[CrossRef](#)]
41. Abioye, A.M.; Ani, F.N. The Characteristics of Oil Palm Shell Biochar and Activated Carbon Produced via Microwave Heating. *Appl. Mech. Mater.* **2014**, *695*, 12–15. [[CrossRef](#)]
42. Ahmad, A.; Loh, M.; Aziz, J. Preparation and characterization of activated carbon from oil palm wood and its evaluation on Methylene blue adsorption. *Dye. Pigment.* **2007**, *75*, 263–272. [[CrossRef](#)]
43. Sun, Y.; Li, H.; Li, G.; Gao, B.; Yue, Q.; Li, X. Characterization and ciprofloxacin adsorption properties of activated carbons prepared from biomass wastes by H₃PO₄ activation. *Bioresour. Technol.* **2016**, *217*, 239–244. [[CrossRef](#)] [[PubMed](#)]
44. Jasper, E.E.; Ajibola, V.O.; Agbaji, E.B.; Onwuka, J.C. Optimization of the preparation of *Millettia thonningii* seed pods activated carbon for use in the remediation of dye-contaminated aqueous solutions. *SN Appl. Sci.* **2019**, *1*, 1351. [[CrossRef](#)]
45. Altintig, E.; Arabaci, G.; Altundag, H. Preparation and characterization of the antibacterial efficiency of silver loaded activated carbon from corncobs. *Surf. Coatings Technol.* **2016**, *304*, 63–67. [[CrossRef](#)]
46. Zhao, Y.; Wang, Z.Q.; Zhao, X.; Li, W.; Liu, S.X. Antibacterial action of silver-doped activated carbon prepared by vacuum impregnation. *Appl. Surf. Sci.* **2013**, *266*, 67–72. [[CrossRef](#)]
47. El-Gendy, N.S.; Madian, H.R.; Amr, S.S.A. Design and Optimization of a Process for Sugarcane Molasses Fermentation by *Saccharomyces cerevisiae* Using Response Surface Methodology. *Int. J. Microbiol.* **2013**, *2013*, 1–9. [[CrossRef](#)]
48. Senthilkumaar, S.; Varadarajan, P.R.; Porkodi, K.; Subbhuraam, C.V. Adsorption of methylene blue onto jute fiber carbon: Kinetics and equilibrium studies. *J. Colloid Interface Sci.* **2005**, *284*, 78–82. [[CrossRef](#)]
49. Zamani, A.H.; Abdullah, N.H. Modeling and optimization of carbon dioxide methanation via in situ hydrogen generated from aluminum foil and alkaline water by Box–Behnken design. *J. Taiwan Inst. Chem. Eng.* **2018**, *82*, 156–162. [[CrossRef](#)]
50. Myers, R.H.; Montgomery, D.C.; Anderson-Cook, C.M. *Response Surface Methodology: Process and Product Optimization Using Designed Experiments*, 4th ed.; Wiley: Hoboken, NJ, USA, 2016.